



Geometrical analysis of thermo-compressors in multiple-effects distillation units based on the second law of thermodynamics

Ramin Kouhikamali^{a,*}, Hosein Sadeghi^a, Ali Safari^a, Navid Sharifi^b

^aDepartment of Mechanical Engineering, University of Guilan, Rasht, Iran

Tel. +98 131 6690276; Fax: +98 131 6690273; email: kouhikamali@guilan.ac.ir

^bDepartment of Aerospace Engineering, University of Amir-Kabir, Tehran, Iran

Received 7 July 2012; Accepted 27 May 2013

ABSTRACT

Thermo-compressors are used instead of mechanical compression devices in many industries and play a main role in the process. Through the process of designing desalination systems, amount of exergy dissipation is a very important economical factor. Most of the exergy losses in multi-effect distillation systems with thermal vapor compression (multiple-effect desalination–TVC) occur in the thermo-compressor. The aim of this article is to investigate geometrical effects in thermo-compressors by numerical methods based on the second law of thermodynamics to obtain lower exergy loss and consequently, higher entrainment ratio. A lot of geometrical parameters such as converging and diverging angles in mixing section, diffuser, nozzle location and also its throat area ratio affect thermo-compressors' performance. The modifications in the above-mentioned parameters were applied to a thermo-compressor established in a desalination unit in Kavian petrochemical company which is working with 15 barg of motive pressure. Numerical simulation of the base model has an accurate agreement with experimental data with about 1.3% discrepancy in maximum discharge pressure and just 6.7% in entrainment ratio. Results of the analysis indicate that thermo-compressor's performance is sensitive to the mixing area converging angle. The other parameter which mostly affects the performance is the location of nozzle in thermo-compressor's body.

Keywords: Thermo-compressor; Geometrical analysis; Exergy analysis; Multiple-effect distillation

1. Introduction

Thermo-compressors and ejectors are widely used in many industries such as multiple-effect desalination (MED) systems to produce vacuum and compression according to specified discharged pressure. Because of the importance of thermo-compressors and also high amount of exergy loss in comparison to other parts of

the unit, the optimization of these devices is vital for better productivity of the system. The optimized thermo-compressor must be designed to increase the amount of the entrainment ratio and decrease exergy destruction and energy consumption. Hence, the flow pattern inside the device should be investigated. Numerical methods are usually useful to reveal different flow patterns inside the thermo-compressor.

Several researches have been done about the performance of thermo-compressors in desalination

*Corresponding author.

systems during the last decade. Exergy analysis of MED–TVC desalination system was performed by Choi et al. [1]. It was found that most of the specific exergy losses in the system occur in TVC and in the effects which account for more than 70% of the total amount. TVC has been accurately designed through the CFD analysis for the various shape parameters and various boundary conditions by Park et al. [2]. Sriveerakul et al. [3,4] investigated the usage of CFD in predicting the performance of a steam ejector used in refrigeration applications. Choke flow, mixing behavior, jet core effect, and the presence of oblique shock were also discussed. A computer simulation code was developed by Kouhikamali et al. to simulate the MED–TVC process [5]. Thermodynamical aspects and an optimization procedure in a case study is presented by them as well [6,7]. The first attempt to tackle two-phase aspect was also performed numerically by Sharifi et al. [8]. A geometrical modification of a thermo-compressor in a MED system was done by Kouhikamali et al. [9]. It was shown that the entrainment ratio is very sensitive to the geometrical parameters of mixing area zone and throat section of the thermo-compressor.

This article focuses on different effects of geometry and on the performance of thermo-compressor. A study based on energy and exergy considerations is conducted to observe how the entrainment ratio and the amount of exergy losses change with modification in geometrical parameters. A thermo-compressor which is currently working in MED units in Assaluyeh in south of Iran was considered as the base model and simulated by CFD code. The results were confirmed approximately with experimental data. Moreover, it is shown how the entropy generation and the entrainment ratio are changed by modifying the converging angle of mixing area, diverging angle, and outlet diameter of diffuser and nozzle location.

2. Thermo-compressor theory

In general, the thermo-compressor in MED–TVC units is a device to compress a part of the vapor leaving the evaporators from the low pressure to the higher pressure entering the first stage by using a high-pressure steam. As shown in Fig. 1, a typical thermo-compressor consists of four parts: supersonic nozzle, mixing area section, constant area section, and the diffuser.

The motive steam is expanded through a convergent–divergent nozzle and consequently a low-pressure and high-velocity flow is exited from the nozzle as a supersonic jet. This high-velocity steam

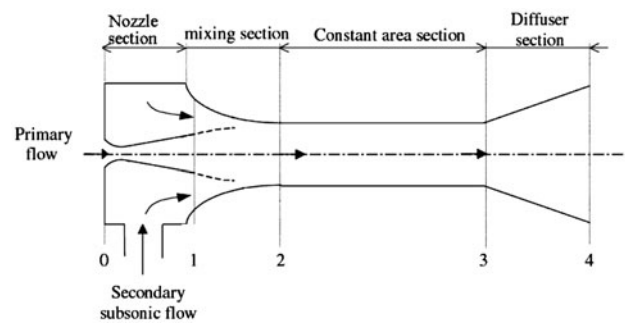


Fig. 1. A scheme of the thermo-compressor with four different parts.

sucks a part of vapors leaving the evaporator. The supersonic steam and sucked vapor mix with each other in the mixing section in the thermo-compressor. The velocity decreases gradually during the mixing phenomenon and after a normal shock occurrence, the kinetic energy is converted into the pressure. Finally, the mixture flows through the diffuser and exits with a pressure higher than the suction pressure.

Suction pressure (P_s), discharge pressure (P_d), motive pressure (P_m), and suction mass flux (\dot{m}_s) are the most important thermodynamic parameters required to design a thermo-compressor for MED–TVC units. On the other hand, the entrainment ratio (the proportion of suction mass flow rate to motive mass flow rate) is the main effective non-dimensional factor that should be considered during the design of a thermo-compressor.

$$ER = \frac{\dot{m}_s}{\dot{m}_m} \quad (1)$$

As shown in Fig. 2, generally, the thermo-compressor works in one of the double choking, single choking, or

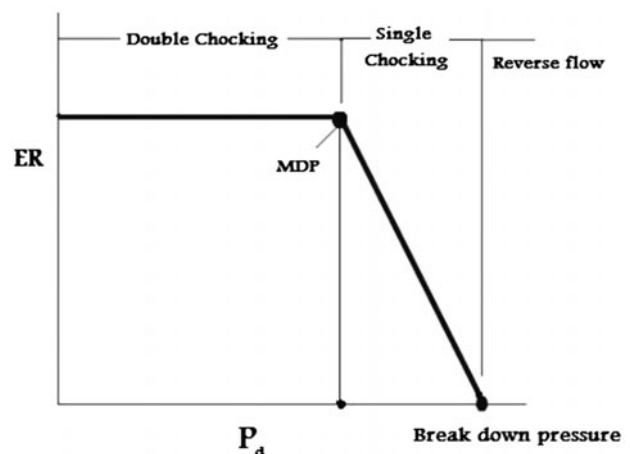


Fig. 2. Operating condition of a thermo-compressor.

reverse flow conditions that occurs in different values of the discharge pressure. Once the discharge pressure is in the range of double choking, the entrainment ratio of the thermo-compressor will remain constant (the desired working condition of a thermo-compressor) prior to the maximum discharge pressure (MDP).

If discharge pressure goes higher, the entrainment ratio will decrease sharply, which shows the thermo-compressor is working in single choking condition. If the discharge pressure reaches the break down pressure, the entrainment ratio will turn into zero and afterwards the thermo-compressor will go to reverse flow condition.

3. Process simulation (CFD model)

The simulation of flow patterns in the thermo-compressor is performed based on the main governing steady equations, conservation of mass (continuity), momentum, and energy, respectively.

$$\frac{\partial(\rho u_i)}{\partial x_i} = 0 \quad (2)$$

$$\frac{\partial(\rho u_i u_j)}{\partial x_i} = \rho g_j - \frac{\partial P}{\partial x_j} + \frac{\partial}{\partial x_i}(\tau_{ij}) \quad (3)$$

$$\frac{\partial(\rho c_p u_i T)}{\partial x_i} = \frac{\partial}{\partial x_i} \left(\lambda \frac{\partial T}{\partial x_i} \right) + \mu \phi \quad (4)$$

In the above equation, τ_{ij} is tension tensor that is defined as:

$$\tau_{ij} = \mu \left(\frac{\partial u_j}{\partial x_i} + \frac{\partial u_i}{\partial x_j} - \frac{2}{3} \delta_{ij} \frac{\partial u_k}{\partial x_k} \right) \quad (5)$$

And $\mu \phi$ is term of viscous dissipation and λ is thermal conductivity.

In addition, 17,000 quadrilateral meshes have been generated to solve continuity, momentum, and energy equations. It should be mentioned that the independency of results to the number of meshes has been checked by the generation of 30,000 quadrilateral meshes, but the result for the entrainment ratio of the base model changed only by 0.6% and the MDP was not changed. Therefore, 17,000 grid was used to solve the equations in this geometry.

The problem was solved as a 2D axisymmetric model with an implicit method and iterating procedure. In order to have accurate results, the residuals were expected to be lower than $1e-6$ and the iteration was continued to reach this limit. Due to supersonic

regimes of steam flow pattern in ejectors, turbulence problem should be considered.

The most common and economical turbulence modeling for compressible flow is “realizable $k-\varepsilon$ model” that is able to predict more accurate spreading rate of a round jet than conventional “standard $k-\varepsilon$ model” [10]. Realizable $k-\varepsilon$ model is expressed as follows:

$$\frac{\partial}{\partial x_j}(\rho u_j k) = \frac{\partial}{\partial x_j} \left[\left(\mu + \frac{\mu_t}{\sigma_k} \right) \frac{\partial k}{\partial x_j} \right] + P_k - \rho \varepsilon \quad (6)$$

$$\frac{\partial}{\partial x_j}(\rho u_j \varepsilon) = \frac{\partial}{\partial x_j} \left[\left(\mu + \frac{\mu_t}{\sigma_\varepsilon} \right) \frac{\partial \varepsilon}{\partial x_j} \right] + \frac{\varepsilon}{k} (c_{\varepsilon 1} P_k - c_{\varepsilon 2} \rho \varepsilon) \quad (7)$$

In these equations p_k and μ_t are given by:

$$P_k = \mu_t \left(\frac{\partial u_i}{\partial x_j} + \frac{\partial u_j}{\partial x_i} \right) \frac{\partial u_i}{\partial x_j} \quad (8)$$

$$\mu_t = c_\mu \rho \frac{k^2}{\varepsilon} \quad (9)$$

and constant values are [10]:

$$c_{\varepsilon 1} = 1.44, c_{\varepsilon 2} = 1.9, \sigma_k = 1, c_\mu = 0.09, \sigma_\varepsilon = 1.2$$

Water vapor, used as the working fluid of the model, was treated as the assumption of an ideal gas. Even though the ideal gas relation seems to be the unrealistic assumption to the model, for the applications where the operating pressure is relatively low, it was proved that this hypothesis provides results similar to the real gas model [11].

For the inlets of the primary nozzle and suction surface, the boundary conditions were set as a constant pressure adopted from a total pressure of the operating state and were fixed at 15 bar and 10 kPa (in absolute scale) for motive and suction steam flows, respectively. The discharge pressure value was considered variant during the simulation to attain the maximum point of normal operation for the thermo-compressor.

4. Thermo-compressor analysis in view of the second law of thermodynamics

Entropy analysis for any thermal system is described as:

$$\Sigma S_{in} - \Sigma S_{out} + S_{gen} = \Delta S_{net} \quad (10)$$



Fig. 3. Experimental MED-TVC units installed in Assalluyeh in Kavian Petrochemical Company [12].

The entropy generation equation may be written as:

$$S_{\text{gen}} = \Sigma S_{\text{out}} - \Sigma S_{\text{in}} \quad (11)$$

Therefore, the rate of entropy generation for the thermo-compressor shown in Fig. 1 with two inlet flows is defined by:

$$\dot{S}_{\text{gen}} = (\dot{m}_m + \dot{m}_s)S_d - \dot{m}_m S_m - \dot{m}_s S_s \quad (12)$$

Another parameter that affects the thermo-compressor performance is the degree of superheating. This parameter is described as the difference between discharge temperature in actual condition and discharge temperature when the process occurs in isentropic condition. The desired demand in thermo-compressor is to convert the kinetic energy of supersonic flow to pressure; but in actual process, a part of this energy causes an increase in outlet temperature instead of pressure.

When the process is isentropic, there is no irreversibility and no entropy generation. Therefore, at isentropic condition, the entropy of that part of outgoing flow which has the partial pressure of suction flow is equal to the entropy of suction flow. It should be mentioned that entering entropy with motive steam flow is not considered as inlet entropy here, because it is considered like a motive work.

$$S_{\text{is}} = S_s \quad (13)$$

The partial discharge pressure of suction flow is defined by:

$$P_p = P_d \left(\frac{\dot{m}_s}{\dot{m}_m + \dot{m}_s} \right) \quad (14)$$

Outlet isentropic temperature (T_{is}) for such isentropic process can be determined by estimated S_{is} and corresponding partial discharge pressure of suction flow. Thus, the degree of superheating can be expressed as:

$$\text{DSH} = T_d - T_{\text{is}} \quad (15)$$

6. Results and Discussion

The effects of geometric parameters such as converging angle of mixing area section, outlet diameter of diffuser, and nozzle location in thermo-compressor were investigated numerically and the CFD calculations were applied to different models. For these models, the entrainment ratio, MDP, entropy generation, and the degree of superheating were obtained numerically and compared in order to improve the performance. In each case, only one parameter has been varied and the others were assumed constant. The main thermo-compressor established in a MED-TVC unit in Kavian Petrochemical Company in Iran which is considered as the base model is shown in Fig. 3 [12].

Fig. 4 shows the variation of the entrainment ratio vs. discharge pressure for the main thermo-compressor which is considered as the base model. The MDP for this model was obtained as 29.6 kPa and the entrainment ratio was calculated as 0.953.

Fig. 5 shows the contours of Mach number for the base model at double choking and single choking

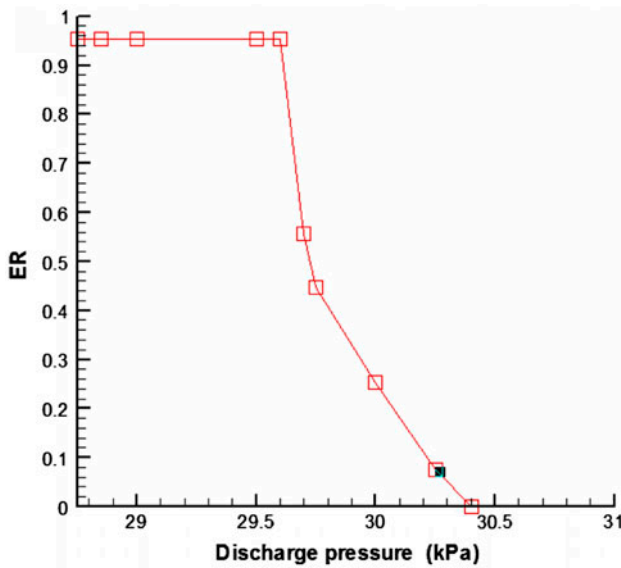


Fig. 4. The variation of entrainment ratio vs. discharge pressure for the base model.

modes. In a double choking mode, a supersonic jet of steam flow is well developed through the mixing duct and a normal shock occurs in the constant area section. It should be noted that if a normal shock phenomenon occurs in the diffuser section, it means the thermo-compressor is over designed and if it occurs in the mixing area section, it means the thermo-compressor will work in an unstable condition with a non-continuous voice. Thus, the thermo-compressor in

this case works in either a single choking or a reverse flow mode.

The entropy generation rate and degree of super heating for the base model at MDP were obtained as 9206.8 ($\frac{W}{K}$) and 62.6°C, respectively.

The modifications in geometrical parameters and comparison with the base model were performed to improve the performance of the thermo-compressor.

Firstly, converging angle of the mixing area was varied due to the change in the inlet diameter of mixing chamber, while its length was assumed to be constant.

The results of the change of performance curves for five models with different inlet diameters were depicted in Fig. 6. As the inlet diameter increases, TVC works with higher entrainment ratio, while the MDP becomes lower.

As can be seen in Fig. 7, it can be concluded that in contrast to the entrainment ratio, the value of the degree of superheating is decreasing by increasing the inlet diameter of mixing chamber.

For instance, when the entrainment ratio is at the peak of the curve, at diameter 86.8 (cm), the degree of superheating has the lowest value.

Fig. 8 shows the relation between the entropy generation and mixing chamber inlet diameter. It is obvious that the entropy generation drops by the growth in the mixing chamber inlet diameter. It should be noticed that the base model has the lowest amount of entropy generation among the others.

Another modification was applied to change the converging angle of the mixing area section. In this

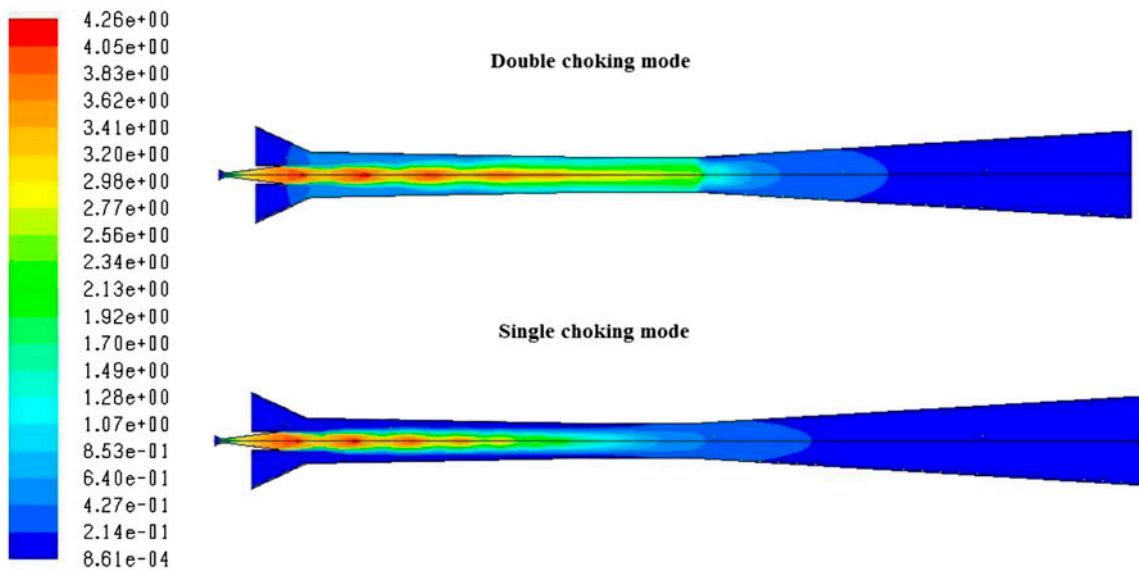


Fig. 5. Contours of Mach number for the base model in double choking and single choking modes.

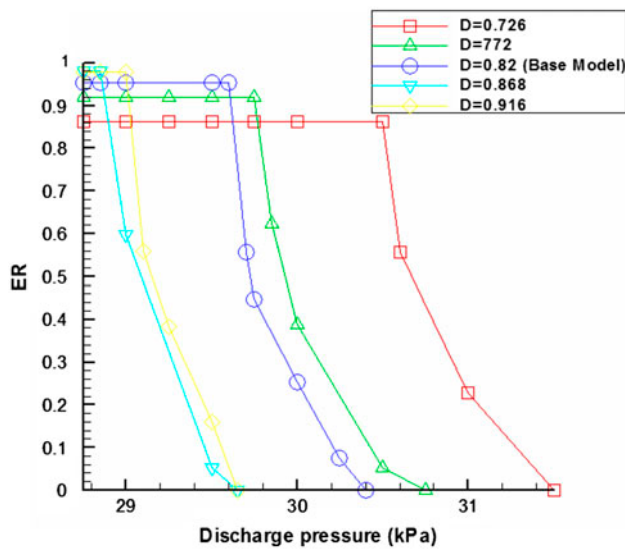


Fig. 6. The variation of entrainment ratio vs. discharge pressure for different inlet diameters of the mixing chamber.

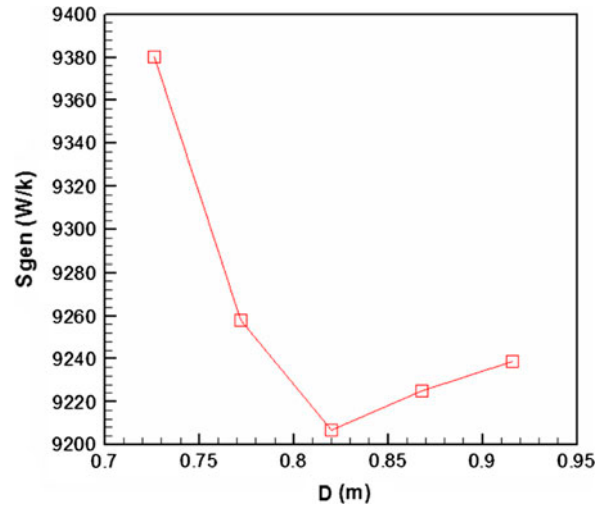


Fig. 8. The entropy generation vs. the mixing chamber inlet diameter.

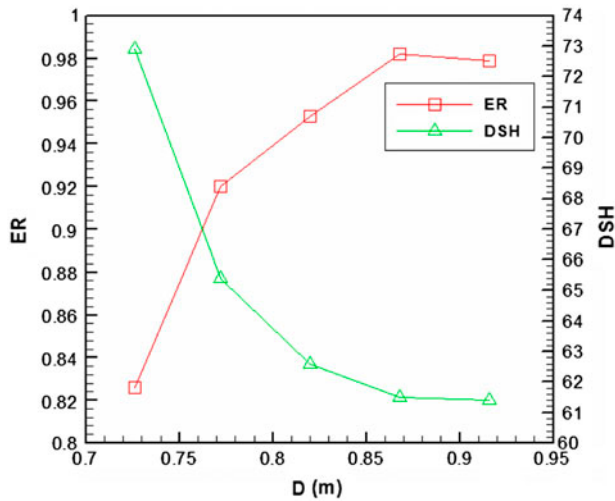


Fig. 7. The entrainment ratio and the degree of superheating vs. the inlet diameter of mixing chamber.

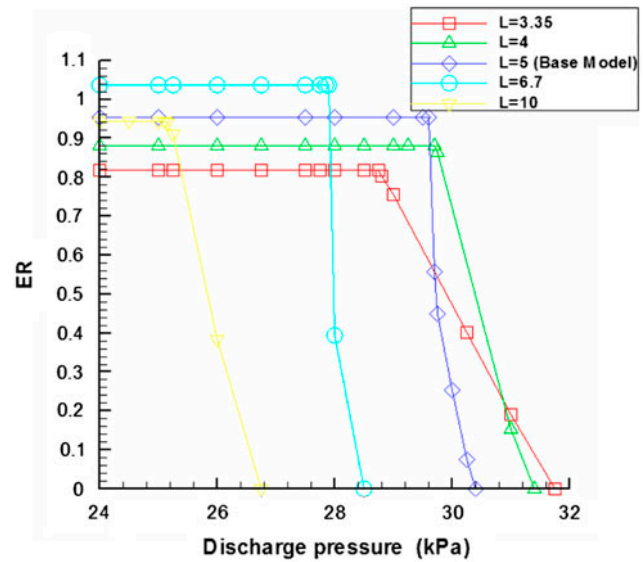


Fig. 9. The variation of entrainment ratio vs. discharge pressure for different lengths of mixing chamber.

case, the inlet diameter of the mixing chamber was assumed constant and its length was altered. As shown in Fig. 9, the entrainment ratio rises by increasing the length of mixing chamber until the length of 6.7 (m) and then starts to decline. But MDP has an inverse result and declines by growth in length.

Fig. 10 shows if the length of mixing chamber increases until 6.7 (m), it results in more entrainment ratio and less degree of superheating. While after that, both of the curves have the inverse trend.

As can be seen in Fig. 11, it can be concluded that the base model has the lowest amount of entropy generation and afterward the entropy generation increases dramatically.

Fig. 12 represents the relation between the entrainment ratio and discharge pressure for five different thermo-compressors with different values of diffuser outlet diameter. This figure illustrates that the variation in diffuser outlet diameter has no significant effect on the entrainment ratio. However, it can be

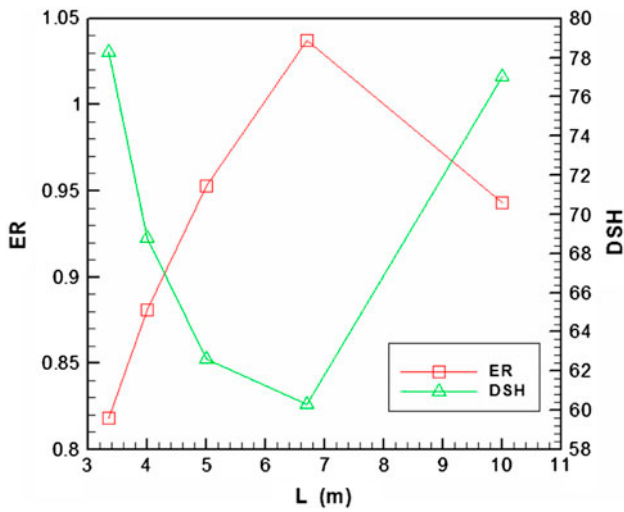


Fig. 10. The entrainment ratio and the degree of superheating vs. the length of mixing chamber.

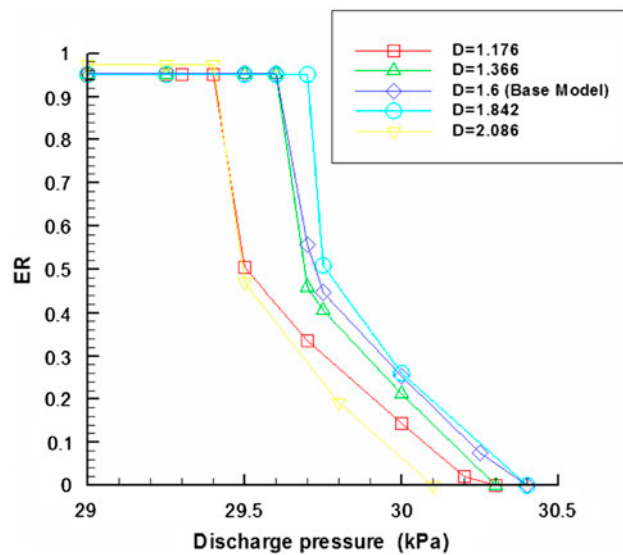


Fig. 12. The variation of entrainment ratio vs. discharge pressure for different outlet diameters of the diffuser.

observed that MDP goes up a little bit by increasing the diameter.

Fig. 13 shows the effect of the nozzle distance from the mixing area on the entrainment ratio and MDP of thermo-compressor. The (X) parameter in the Figure represents the distance between nozzle outlet and mixing chamber inlet. As the nozzle gets closer to the mixing area, the motive steam traverses less in mixing chamber, therefore, lower amount of entropy is generated and a stronger shock occurs. Consequently, the MDP rises. Based on this argument, the portion of

suction flow decreases and the entrainment ratio declines.

Fig. 14 indicates that generally, the degree of superheating has a decreasing trend due to increasing the nozzle distance from the mixing chamber which causes an upward trend in the entrainment ratio.

Fig. 15 shows that the entropy generation increases sharply by increasing the nozzle distance from the mixing chamber.

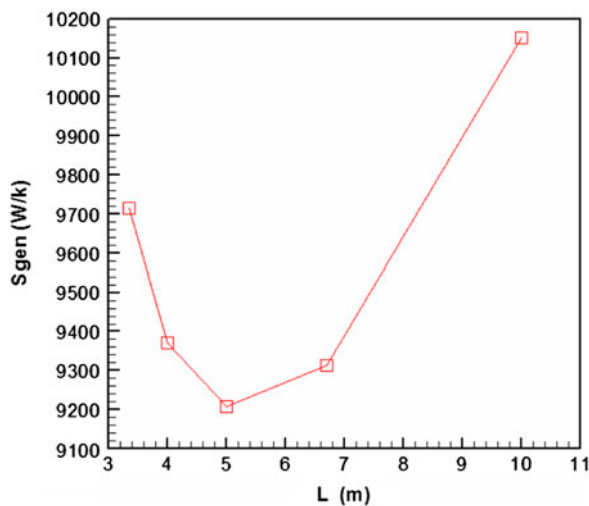


Fig. 11. The entropy generation vs. the length of mixing chamber.

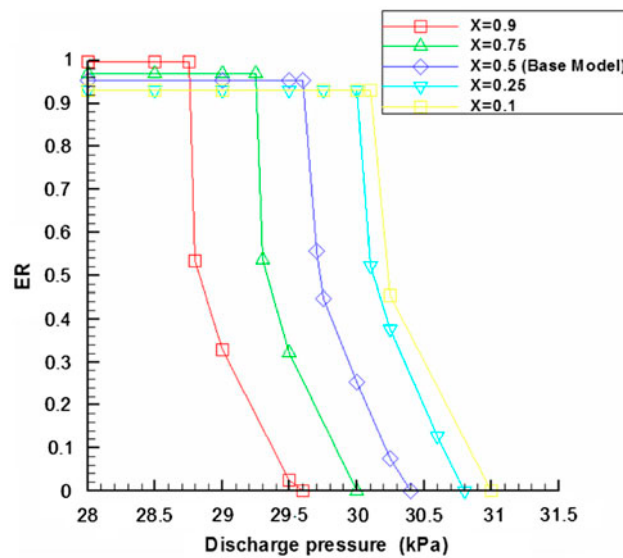


Fig. 13. The variation of entrainment ratio vs. discharge pressure for different nozzle locations.

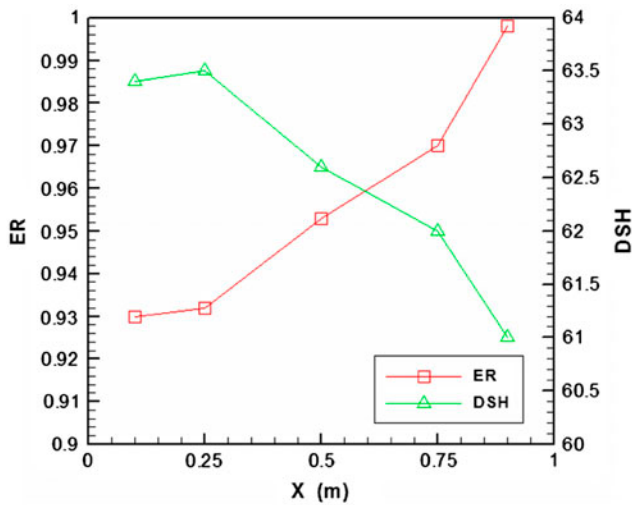


Fig. 14. The entrapment ratio and the degree of superheating vs. the distance of the nozzle from the mixing chamber.

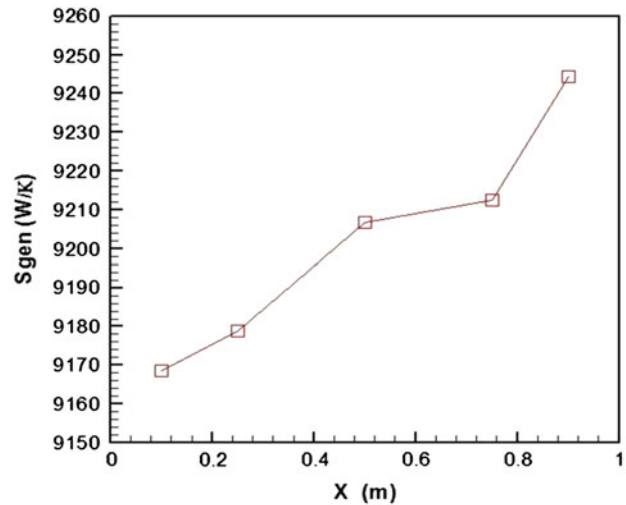


Fig. 15. The entropy generation vs. the distance of the nozzle from the mixing chamber.

7. Conclusion

Finally the following points can be concluded from this research:

- The performance of a thermo-compressor is very sensitive to the change in diameter and length of the mixing area, while alteration in diffuser dimension has no considerable effect on the thermo-compressor performance.
- As the inlet diameter of mixing chamber increases, TVC works with lower entropy generation and lower degree of superheating, which causes an increase in the entrapment ratio.
- In addition, it has been clearly demonstrated that the MDP of the thermo-compressor decreases due to any increase in mixing area length and diameter.
- As the nozzle gets closer to the mixing area, the entropy generation decreases and consequently, the MDP goes up. Moreover, the entrapment ratio declines by decreasing the distance between the nozzle and the mixing chamber.
- The entropy generation and the degree of superheating have the same trend and the entrapment ratio has an inverse trend in comparison to them, except in the nozzle location variations in which, the trends of entropy generation and the degree of superheating are different.

Nomenclature

MDP	—	maximum discharge pressure
ER	—	entrapment ratio
DSH	—	degree of superheating

\dot{m}	—	flow rate
P	—	pressure
S	—	entropy
T	—	temperature
ρ	—	density
u_i	—	velocity
τ_{ij}	—	stress tensor
μ	—	dynamic viscosity
c_p	—	specific heat capacity
D	—	diameter
L	—	length
X	—	distance between the nozzle outlet and mixing chamber inlet
λ	—	thermal conductivity
k	—	turbulent kinetic energy
ε	—	turbulent dissipation rate

Subscripts

s	—	suction
m	—	motive steam
d	—	discharge
p	—	partial
in	—	inlet
out	—	outlet
net	—	total
gen	—	generated
is	—	isentropic

References

- [1] H.S. Choi, J.L. Yang, G.K. Seok, L. Song, Performance improvement of multiple-effect distiller with thermal vapor compression system by exergy analysis, *Desalination* 182 (2005) 239–249.

- [2] I.S. Park, S.M. Park, J.S. Ha, Design and application of thermal vapor compressor for multi-effect desalination plant, *Desalination* 182 (2005) 199–208.
- [3] T. Sriveerakul, S. Aphornratana, K. Chunnanond, Performance prediction of steam ejector using computational fluid dynamics. Part 1: Validation of the CFD results, *Int. J. Therm. Sci.* 46 (2007) 812–822.
- [4] T. Sriveerakul, S. Aphornratana, K. Chunnanond, Performance prediction of steam ejector using computational fluid dynamics. Part 2: Flow structure of a steam ejector influenced by operating pressures and geometries, *Int. J. Therm. Sci.* 46 (2007) 823–833.
- [5] R. Kouhikamali, A. Abbassi, S.A. Sadough, M. Saffar Avval, Thermodynamic design and parametric study of MED–TVC, *Desalination* 222 (2008) 596–604.
- [6] R.K. Kamali, S. Mohebbinia, Experience of design and optimization of multi-effect desalination systems in IRAN, *Desalination* 222 (2008) 639–645.
- [7] R. Kouhikamali, A. Samami Kojidi, M. Asgari, F. Alamolhoda, The effect of condensation and evaporation pressure drop on specific heat transfer surface area and energy consumption in MED–TVC plants, *Desalin. Water Treat.* 46 (2012) 68–74.
- [8] N. Sharifi, M. Boroomand, R. Kouhikamali, Wet steam flow energy analysis within thermo-compressors, *Energy* 47 (2012) 609–619.
- [9] R. Kouhikamali, N. Sharifi, Experience of modification of thermo-compressors in multiple effects desalination plants in Assaluyeh in IRAN, *Appl. Therm. Eng.* 40 (2012) 174–180.
- [10] FLUENT 6.0 User's Guide, vols. 1–5, Fluent, Lebanon, 2001.
- [11] S. Aphornratana, Theoretical and experimental investigation of a combine ejector-absorption refrigerator, PhD thesis, University of Sheffield, UK, 1994.
- [12] www.fanniroo.com